

CRouting: Reducing Expensive Distance Calls in Graph-Based Approximate Nearest Neighbor Search

Zhenxin Li zhenxin@zju.edu.cn Zhejiang University Hangzhou, China	Shuibing He* heshuibing@zju.edu.cn Zhejiang University Hangzhou, China	Jiahao Guo guahao@zju.edu.cn Zhejiang University Hangzhou, China
Xuechen Zhang xuechen.zhang@wsu.edu Washington State University Vancouver, United States of America	Xian-He Sun sun@iit.edu Illinois Institute of Technology Chicago, United States of America	Gang Chen cg@zju.edu.cn Zhejiang University Hangzhou, China

Abstract

Approximate nearest neighbor search (ANNS) is a crucial problem in information retrieval and AI applications. Recently, there has been a surge of interest in graph-based ANNS algorithms due to their superior efficiency and accuracy. However, the repeated computation of distances in high-dimensional spaces constitutes the primary time cost of graph-based methods. To accelerate the search, we propose a novel routing strategy named CRouting, which bypasses unnecessary distance computations by exploiting the angle distributions of high-dimensional vectors. CRouting is designed as a plugin to optimize existing graph-based search with minimal code modifications. Our experiments show that CRouting reduces the number of distance computations by up to 41.5% and boosts queries per second by up to 1.48 \times on two predominant graph indexes, HNSW and NSG. Code is publicly available at <https://github.com/ISCS-ZJU/CRouting>.

1 Introduction

Approximate nearest neighbor search (ANNS) finds wide application in areas such as information retrieval [24, 82], image and video analysis [8], key-value storage [66], and recommender systems [65], where quick retrieval for the most similar K items is crucial (known as the *top- K* problem). In particular, driven by recent advancements in large language models (LLMs), ANNS services have become a core component of modern AI infrastructure [47]. Domain knowledge from various data formats (e.g., documents, images, and speech) is embedded and stored as high-dimensional feature vectors. When a user queries a chatbot, the ANNS engine retrieves semantically similar vectors, delivering relevant contexts to enhance the response quality of LLMs.

The retrieval of exact nearest neighbors in high-dimensional spaces is computationally expensive due to the curse of dimensionality [41]. To address this, ANNS offers a practical trade-off by returning an approximate set of the K nearest neighbors within an acceptable error margin, thereby achieving efficient scalability for high-dimensional data. Based on the index structure, the existing ANNS algorithms can be divided into four major categories, including tree-structure based approaches [11, 12, 16, 19], hashing-based approaches [20, 27, 50, 53], quantization-based approaches [7, 8, 31, 34], and graph-based approaches [25, 26, 54, 55].

*Shuibing He is the corresponding author.

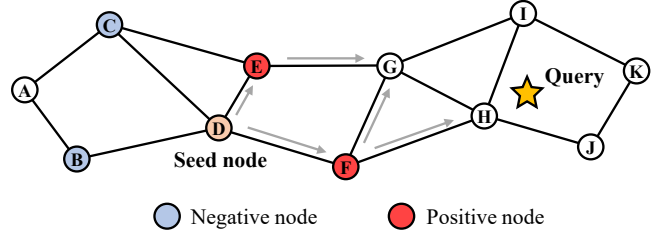


Figure 1: Illustration of the greedy search algorithm.

Among these, graph-based algorithms, such as HNSW [55] and NSG [26], have shown promising search performance over other approaches [52, 75]. They efficiently explore neighborhood structures by constructing a graph where nodes represent feature vectors and edges denote potential nearest neighbor relationships. Graph-based methods scale effectively with large datasets and adapt well to various data distributions. As a result, they form the foundation of various ANNS services and vector databases, including Elasticsearch [35], FAISS [45], Milvus [73], VSAG [81], and PostgreSQL [78].

The graph-based ANNS algorithms commonly use the greedy search algorithm for searching nearest neighbors. As shown in Figure 1, it maintains a candidate set where candidates are assessed based on their distance from the query point. Starting from the specified seed node, each candidate's neighbors are examined. Neighbors whose distances to the query exceed the farthest distance in the candidate set are discarded (i.e., negative nodes), while others are included in the candidate set and further refined (i.e., positive nodes). The iterative distance calculation calls find nodes closer to the query, progressively moving towards the query point.

However, repeated distance calculations in high-dimensional spaces are costly and constitute the primary time bottleneck in ANNS. For example, our experiments show that distance calculations account for at least 83% of the total running time across five widely used datasets with varying sizes and dimensionalities (§2.2). Furthermore, the majority of nodes involved in these calculations are negative objects, meaning they will not be included in the candidate set and do not affect the final result. Based on these observations, it suggests that developing a method to prune negative nodes could reduce expensive distance calculations without compromising accuracy.

Various routing techniques are proposed to improve the performance of graph-based ANNS. The primary objective is to minimize distance computations during neighbor exploration. For example, HCNNG [58] and TOGG [76] employ KD-trees [11] to select points in the same direction as the query thereby only exploring a subset of neighbors for each search iteration. However, they tend to yield suboptimal query accuracy because of incorrect pruning, limiting their effectiveness. FINGER [15] pre-computes and stores the residual vectors for all nodes' neighbors during construction, allowing for rapid distance estimation and node pruning during search. Other ML-based optimizations [10, 48, 61] learn routing functions, utilizing additional representations to facilitate optimal routing from the starting node to the nearest neighbor. However, all these optimizations either compromise search accuracy or necessitate additional training and extra information, leading to increased construction time and memory footprint.

In this paper, we propose CRouting, a novel routing strategy to guide the navigation for graph-based ANNS. Compared to existing routing strategies, CRouting achieves a favorable balance between search and construction efficiency. CRouting takes inspiration from the characteristics of high-dimensional vector distribution: *in high-dimensional spaces, two random vectors are almost always very close to orthogonal* [9]. Following this theorem, in the triangles formed by the current search node, the query node, and the neighboring node, we observe that the angles associated with the current search node tend to concentrate around a specific value. Based on this observation, CRouting uses the cosine theorem to efficiently estimate the distance between the neighbor node and the query node. The estimated distance is used to decide whether to prune the neighbor, thereby reducing unnecessary computational overhead. Since the estimated distance may have approximation errors, some nodes might be incorrectly pruned. CRouting further introduces a technique to identify these incorrectly pruned nodes and recalculate their exact distances to the query to ensure high accuracy. In summary, this paper makes the following contributions:

- We conduct a thorough analysis of existing graph-based ANNS algorithms and find that all of them are plagued by repeated distance computations, which account for the majority of the overall search operation costs.
- We propose CRouting, a novel routing strategy that guides navigation by leveraging the characteristics of high-dimensional vector distributions. Collaborated with an error-correction technique, CRouting effectively prunes massive unnecessary distance computations under the same accuracy criteria.
- We implement CRouting and develop it as a plugin to enhance HNSW and NSG, two predominant graph-based ANNS algorithms. Our evaluation results show that CRouting reduces the number of distance computations by up to 41.5% while maintaining the same accuracy, thereby improving queries per second (QPS) by up to 1.48×.

2 Background and Motivation

2.1 Greedy Search

The greedy search algorithm is commonly used in most graph-based methods for finding nearest neighbors. As shown in Algorithm 1,

Algorithm 1 Greedy Search

```

Input: query  $q$ , starting point  $p$ , candidate neighbor limit  $efs$ 
Output: top results queue  $T$ 
1: candidate queue  $C = \{p\}$ ,  $T = \{p\}$ , mark  $p$  as visited
2: while  $C$  is not empty do
3:    $c \leftarrow$  nearest element from  $C$  to  $q$ 
4:    $upper\ bound \leftarrow$  farthest element distance from  $T$  to  $q$ 
5:   if  $dist(c, q) > upper\ bound$  then
6:     return  $T$ 
7:   for each point  $n \in$  neighbors of  $c$  do
8:     if  $n$  is visited then
9:       continue
10:      mark  $n$  as visited
11:      if  $dist(n, q) < upper\ bound$  or  $|T| < efs$  then
12:         $C.add(n)$ ,  $T.add(n)$ 
13:      if  $|T| > efs$  then
14:         $T.resize(efs)$ , update  $upper\ bound$ 
15:   return  $T$ 

```

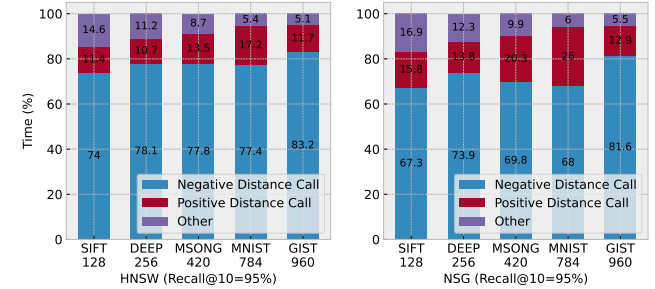


Figure 2: Running time analysis of the greedy search across five datasets with dimensions ranging from 128 to 960.

given a query point q and a starting point p , the algorithm is designed to search for efs nearest neighbors to q . It maintains two priority queues: candidate queue C that stores potential candidates to expand and top results queue T that stores the current most similar candidates. At each search iteration, it first extracts the current nearest point c in C and gets the furthest distance to the query q from T as an *upper bound* (lines 3-4). And then it visits c 's neighbors and computes their distance to q respectively to expand the candidates. For each neighbor, it checks whether its distance from q is less than the *upper bound* and if so, it pushes the neighbor into both C and T , and updates the *upper bound* simultaneously (lines 11-14). The repeated distance calls constitute the primary time cost (line 11).

2.2 Running Time Analysis

We measure the time consumption of greedy search across five public datasets using two state-of-the-art graph-based ANNS algorithms: HNSW and NSG. In this test, if a node is added to the candidate queue after triggering a distance calculation, we refer to it as a positive node; otherwise, it is termed a negative node.

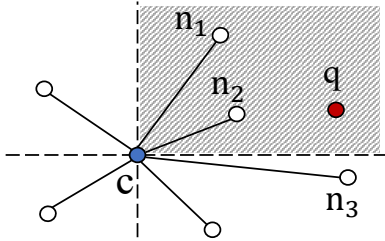


Figure 3: Optimized guided search in TOGG. Only the neighbors in the same direction as the query node q will be considered, such as n_1 and n_2 . However, this can easily overlook potentially valuable nodes, such as n_3 .

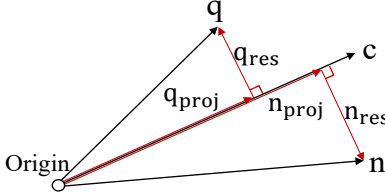


Figure 4: Decomposition of the distance computation in FINGER. The query node q and the neighbor node n can be represented by vectors parallel and orthogonal to the node c .

Table 1: Comparison between different routing strategies.

Strategy	Construction time	Memory footprint	Accuracy
TOGG	Fast ✓	Low ✓	Low ✗
FINGER	Slow ✗	High ✗	High ✓
CRouting	Fast ✓	Low ✓	High ✓

As shown in Figure 2, when the data dimensionality increases from 128 to 960, the proportion of time spent on distance calculations rises from 85.4% to 94.9% on the HNSW algorithm, and from 83.1% to 94.5% on the NSG algorithm, respectively. Moreover, we observe that the majority of nodes are negative, indicating that these nodes will not be added to the candidate set and will not have any further impact on the final result. This suggests that if we can develop a method to prune these negative nodes, we could significantly reduce expensive distance calculations without compromising accuracy.

2.3 Existing Routing Strategies

Several routing techniques have been proposed to minimize distance computations during neighbor exploration. Here, we describe two state-of-the-art routing strategies, including TOGG and FINGER, which we use in the experimental section for comparison with CRouting.

TOGG introduces a two-stage routing strategy that combines optimized guided search with a greedy algorithm. The routing process is explicitly divided into two detailed stages: (S1) the routing stage that is farther from the query and (S2) the routing stage that is closer to the query. In stage S1, the primary focus is on quickly identifying the neighborhood of the query to enable prompt

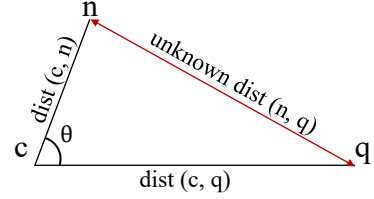


Figure 5: Triangle formed by the current search node c , a query q , and a specific neighbor of c , referred to as n . Our object is to estimate $dist(n, q)$ with low cost.

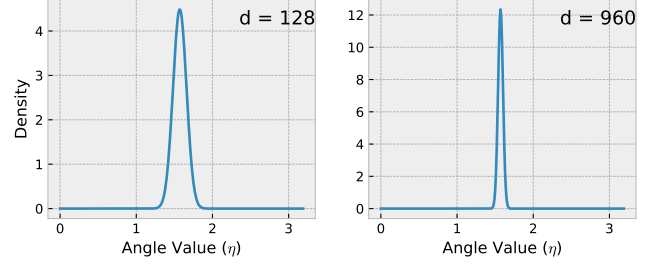


Figure 6: Probability density of angles between two random vectors, where d represents the vector dimension.

routing toward it. To achieve this, TOGG utilizes KD-trees to select points aligned with the query direction, thereby allowing it to explore only a subset of neighbors during each search iteration, as illustrated in Figure 3. In contrast, stage S2 emphasizes the need to thoroughly explore vertices near the query in order to obtain sufficiently accurate search results. Consequently, this stage not only examines the neighbors of each vertex in the candidate set but also investigates the neighbors of those neighbors. By relaxing the expansion constraint compared to traditional greedy algorithms, TOGG effectively mitigates the risk of getting trapped in local optima. However, the utilization of KD-trees for navigation may result in reduced accuracy, as numerous potential nodes are filtered out during stage S1 and cannot be reintegrated in stage S2.

FINGER estimates the distance between each neighbor and the query. Specifically, for each node, it generates projected vectors locally for both neighbors and the query to define a subspace, and then applies Locality Sensitive Hashing (LSH) [14] to approximate the residual angles. As illustrated in Figure 4, the distance is decomposed as follows:

$$\|q - n\|^2 = \|q_{proj} - n_{proj}\|^2 + \|q_{res}\|^2 + \|n_{res}\|^2 - 2q_{res}^T n_{res} \quad (1)$$

During graph construction, FINGER will calculate and store $\|c\|$ (1 byte), $\|n_{res}\|$ (4 bytes), projection coefficient b ($b = \frac{\|n_{proj}\|}{\|c\|}$, 4 bytes), and other relevant LSH information for estimating the angle between q_{res} and n_{res} . Then, FINGER can quickly estimate distances and eliminate unnecessary calculations during query processing. However, this method necessitates additional computation and supplementary information, leading to increased time and memory overhead for graph construction.

Existing routing strategies either compromise search accuracy or require additional construction overhead. In contrast, CRouting

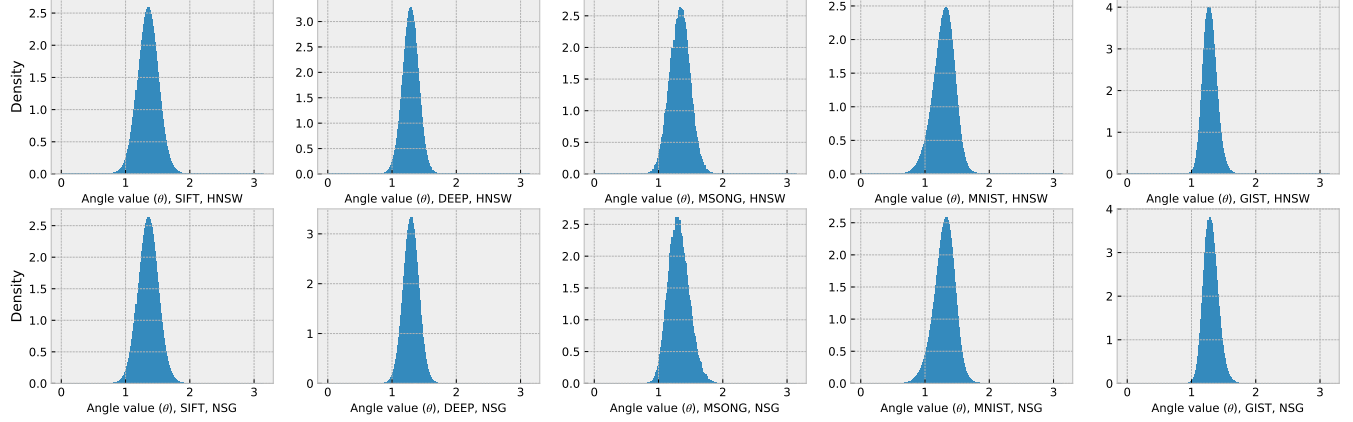


Figure 7: Probability density of angles on HSNW and NSG algorithms. The number of queries is 0.1% of the dataset size.

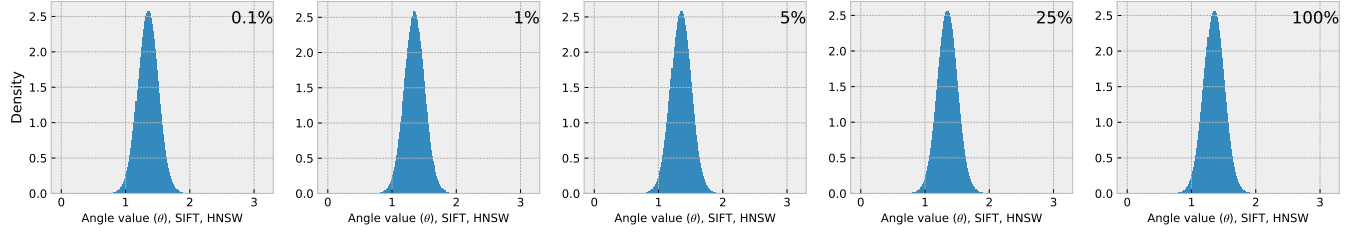


Figure 8: Probability density of angles on HNSW algorithm. The number of queries varies from 0.1% to 100% of the dataset size.

strikes a favorable balance between search and construction efficiency. Table 1 compares CRouting with existing routing strategies, and the detailed experimental results are presented in §5.7.

3 Problem Definition and Analysis

In this section, we present the insight behind CRouting, an effective distance estimation method that leverages the characteristics of high-dimensional vector distributions.

3.1 Problem Statement

As shown in Figure 5, during each search iteration, given a query q , a current search node c , and a specific neighbor of c called n , traditional greedy search algorithms compute the exact Euclidean distance between q and n (i.e., $dist(n, q)$), with a time complexity of $O(d)$, where d is the data dimension. Our objective is to approximate this distance. If the estimated distance exceeds the *upper bound* (i.e., the furthest distance to the query q from the top results queue T as stated in Algorithm 1), then node n can be pruned. This approach ensures that only nodes with a potential to be closer to the query q are considered, thus optimizing the search process and reducing computational overhead.

3.2 Naive Solution: Triangle Inequality

Currently, we only know $dist(c, q)$ because c is extracted from the candidate queue, and $dist(c, q)$ is pre-calculated in a previous search iteration. However, this information alone is insufficient to estimate

$dist(n, q)$. Note that n is a neighbor of c , so $dist(c, n)$ was calculated during the graph construction and can be retained in memory.

After obtaining the exact lengths of the edges (i.e., $dist(c, q)$ and $dist(c, n)$), we can directly apply the triangle inequality to estimate the lower bound of the third edge's length. Specifically, in $\triangle ncq$:

$$dist(n, q) \geq |dist(c, n) - dist(c, q)| \quad (2)$$

And if $|dist(c, n) - dist(c, q)|$ is greater than the *upper bound*, we can directly prune node n . However, our research shows that this method is not always effective. For instance, it reduces the number of distance computations by only 0.08% using the SIFT dataset on the HNSW algorithm, which is negligible in the overall search process. Although the triangle inequality provides an accurate lower bound, it is often too loose to effectively filter out nodes.

3.3 Optimized Solution: Cosine Theorem

To obtain a more accurate distance estimation, additional information, the angle $\angle ncq$ (θ in Figure 5), is required. With this angle, we can then calculate $dist(n, q)$ using the cosine theorem.

The distribution of vectors in high-dimensional spaces has a unique property: *in high-dimensional spaces, two random vectors are almost always very close to orthogonal*. The probability density function of the angle η between two randomly selected vectors can be formulated as follows:

$$P(\eta) = \frac{\Gamma\left(\frac{d}{2}\right)}{\Gamma\left(\frac{d-1}{2}\right)\sqrt{\pi}} \sin^{d-2} \eta \quad (3)$$

where d is the dimensionality of the vector and $\Gamma()$ is the Gamma function. This indicates that the angle distribution is solely determined by the dimensionality of the vectors. To better understand, Figure 6 plots the probability density for $d = 128$ and $d = 960$. As d increases, the values of η become increasingly concentrated around 0.5π (orthogonal).

Inspired by this, we question whether the angle θ between vectors \vec{cn} and \vec{cq} in Figure 5 satisfies the above equation. Because the position of neighbor n is completely random with respect to the current node c , the direction of vector \vec{cn} relative to \vec{cq} is independent. Therefore, the values of angle θ may also exhibit special distribution characteristics.

To further verify this, we record the values of θ along the search paths across different datasets and algorithms using randomly generated queries. The number of queries varies from 0.1% to 100% of the number of nodes to construct the graph. From the results in Figure 7 and Figure 8, we have the following observations. (1) We observe that the values of θ follow a skewed distribution, with the center around 0.5π , which is similar to the trend shown in Figure 6. (2) We observe that the distribution of angles is determined solely by the dataset and remains unaffected by the graph construction algorithm or the number of query nodes. This indicates that the angle distribution is an intrinsic property of the dataset. Because the dataset's vector dimensionality and distribution remain constant, the angle distribution can be used indefinitely once computed.

Based on these observations, we propose the key design concept of CRouting. For each dataset, CRouting selects a specific angle derived from its angle distribution (i.e., the central point) to set the value of θ in the cosine theorem. Given that the angle exhibits a skewed characteristic, using a single representative value for all the angle values along the search path enables a efficient estimate of $dist(n, q)$ while keeping the distance estimation error within a small range.

4 CRouting Design

This section describes the graph construction and query processes of CRouting. CRouting is designed as a plugin to improve the query performance of existing graph-based ANNS algorithms.

4.1 Graph Construction

Acquisition of additional information. As a prerequisite for CRouting, we need to obtain two additional pieces of information during graph construction: (1) the distances between each node and all its neighbors, and (2) the angle distribution of θ . The distances between each node and its neighbors are already calculated during the graph construction process in all the existing graph-based ANNS algorithms. CRouting simply saves them in memory rather than discarding them. To obtain the angle distribution, we will randomly generate n_{sample} query nodes after the graph has been constructed. On the search paths of these nodes, we simultaneously use the cosine theorem to calculate the angle values.

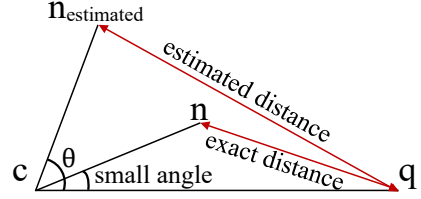


Figure 9: Example of incorrect estimation.

Extra time overhead. By default, the value of n_{sample} is set to 0.1% of the number of nodes used to construct the graph. Because the sampling frequency is sufficient to obtain an accurate angle distribution (as shown in Figure 8), while the computational overhead remains negligible. Our experiments show that the additional construction time does not exceed 4% (§5.7).

Extra memory overhead. One concern is that storing distances between neighbors incurs extra memory overhead. In graph-based ANNS algorithms, memory is used for storing high-dimensional vectors, graph indexs, and distance values (mem_{dist}) saved by CRouting. Our study shows that mem_{dist} leads to an additional 2% to 21% overhead compared to the approaches without using CRouting (§5.7). The ratio of additional memory consumption is decreased as the dimensionality of datasets is increased.

4.2 Graph Search

Pruning strategy. By utilizing the stored $dist(c, n)$ and $dist(c, q)$, along with the angle θ obtained from the distribution of high-dimensional random vectors (§3.3), we can efficiently estimate $dist(n, q)$ using the cosine theorem. If $dist(n, q)$ is not less than the *upper bound*, we can avoid making the expensive distance call to calculate the exact distance. Otherwise, the normal routing process will proceed as usual. Adjusting the angle θ allows us to control the threshold for the pruning strategy. Specifically, larger angle values lead to more nodes being pruned, but they also increase the estimation error, impacting accuracy. Thus, there is a trade-off between accuracy and the number of distance calculations. We evaluate it in detail in §5.5.

Error correction. Although many unnecessary nodes can be effectively pruned, a significant issue remains. Our pruning strategy may introduce approximation errors, which may lead to the removal of important nodes and notably impact the final results. For instance, as illustrated in Figure 9, given a query q and the current search node c , we expand the search by exploring the neighbors of c . The specific neighbor node n , which lies in the direction of q (i.e., with an extremely small angle), is closer to q than c , making it a strong candidate for refining the final results. However, for such neighbors, the error in our estimated distance compared to the actual distance can be significant, raising the likelihood that these promising nodes are mistakenly pruned. Additionally, the convergence paths from these neighbors may also be overlooked, negatively impacting accuracy.

To address this issue, we devise an error correction mechanism to identify erroneously deleted nodes. The key idea is that nodes mistakenly pruned and located near the query node are likely to be revisited in subsequent searches because of the graph's connectivity. This means that even if some positive nodes are pruned initially,

Algorithm 2 Graph Search of CRouting

Input: query q , starting point p , candidate neighbor limit efs
Output: top results queue T

- 1: candidate queue $C = \{p\}$, $T = \{p\}$, mark p as visited
- 2: **while** C is not empty **do**
- 3: $c \leftarrow$ nearest element from C to q
- 4: $upper\ bound \leftarrow$ farthest element distance from T to q
- 5: **if** $dist(c, q) > upper\ bound$ **then**
- 6: **return** T
- 7: **for** each point $n \in$ neighbors of c **do**
- 8: **if** n is visited **then**
- 9: continue
- 10: **if** n is not pruned and $|T| \geq efs$ **then**
- 11: **if** $appx_dist(n, q) \geq upper\ bound$ **then**
- 12: mark n as pruned
- 13: continue
- 14: mark n as visited
- 15: **if** $dist(n, q) < upper\ bound$ or $|T| < efs$ **then**
- 16: $C.add(n)$, $T.add(n)$
- 17: **if** $|T| > efs$ **then**
- 18: $T.resize(efs)$, update $upper\ bound$
- 19: **return** T

they can still be reached through alternative paths in later stages of the search. For example, as shown in Figure 1, if node G is pruned while evaluating the neighbors of node E , it will still be revisited when expanding from node F . Based on this idea, if a node has been pruned by CRouting, any future access to that node should involve calculating its exact distance to ensure high accuracy.

Put it all together. Algorithm 2 describes the graph search process of CRouting. Compared to the existing ANNS algorithms using greedy search (e.g., Algorithm 1), CRouting uses the approximated distance to aggressively prune nodes (lines 10-13) before each exact distance calculation (line 15). Errors may happen when a node is marked as “pruned” (line 12). In this case, when the node is revisited in the future search, CRouting will mark the node n as “visited” and calculate the exact $dist(n, q)$ (lines 14-15). We design CRouting as a plug-in that can be applied on top of any existing graph-based ANNS algorithms that utilize greedy search, requiring only minimal changes to the existing code.

4.3 Applicability to Other Distance Metrics

In addition to Euclidean distance, CRouting can be easily extended to two other commonly used distance metrics: inner-product and cosine distance, through simple transformations. For a query q and data point c with an angle θ between them, the inner-product distance is given by: $IPDist(c, q) = 1 - \|c\| \|q\| \cos\theta$. The relationship between Euclidean and inner product distance is:

$$\begin{aligned} EuclideanDist(c, q)^2 &= \|c\|^2 + \|q\|^2 - 2\|c\|\|q\|\cos\theta \\ &= \|c\|^2 + \|q\|^2 + 2IPDist(c, q) - 2 \end{aligned} \quad (4)$$

Since the calculation of $\|q\|$ is a one-time operation for each query, it remains computationally inexpensive. Moreover, $\|c\|$ (i.e., the norm for each inserted vector) can be precomputed and stored during the graph construction phase. The associated space and time

Table 2: Data statistics.

Dataset	# Base	# Query	# Dim	Type
SIFT [1]	1,000,000	10,000	128	Image
DEEP [3]	1,000,000	1,000	256	Image
MSONG [2]	992,272	200	420	Audio
MNIST [46]	60,000	10,000	784	Image
GIST [1]	1,000,000	1,000	960	Image

costs are acceptable. Specifically, the space required for storing the norm of a vector (typically with dimensions greater than 100) is less than 1%. The computational cost of calculating the norm one time is negligible compared to the numerous distance calculations required for graph construction. In addition, the cosine distance is equivalent to the inner-product distance on normalized data and query vectors [28], where CRouting is still applicable. We evaluate the generality of CRouting in §5.6.

5 Evaluation

Our experiments involve three folds. First, we compare our methods with traditional graph-based approaches to empirically demonstrate that CRouting can be integrated into graph-based greedy search methods for improved performance. Second, we evaluate the sensitivity, generality, and scalability of CRouting in various scenarios. Third, we compare our methods with other routing strategies to assess their efficiency and effectiveness.

5.1 Experimental Setting

Implementation setup. We run the experiments on a Linux server with two Intel Xeon Gold 5318Y CPUs. Each CPU has 24 physical/48 logical cores, 64 GB DRAM. All source codes are compiled with g++10.3 with -O3 optimization. Following previous work [28, 52, 75], we disable all hardware-specific optimizations such as SIMD and memory prefetching so as to focus on the comparison among algorithms themselves. To improve construction efficiency, the code involving vector calculation is parallelized for the index construction. All tests are evaluated on a single thread by default.

Datasets and metrics. We use five public datasets with varying sizes and dimensionalities, detailed in Table 2. They are commonly employed to benchmark ANNS algorithms [6]. We use the Euclidean distance as the distance metric by default. The comparison metrics used to evaluate performance are: (1) Recall@K: it measures search accuracy by comparing the approximate point set T found for a given query q with the true K nearest neighbor result set R . It is defined as: $Recall@K = |T \cap R|/K$. By default, K is set to 10. (2) QPS: it indicates the number of queries a machine can handle per second. (3) Speedup in distance calls [15, 74, 76]: it measures the efficiency of a method by comparing the number of distance calculations. It is defined as the ratio of distance calculations in the brute-force method to those in the optimized routing method. Since the accuracy and performance of greedy search can vary on the size of the candidate array efs (see Algorithm 1), we adjust efs to plot both the recall-QPS curve and the recall-speedup curve.

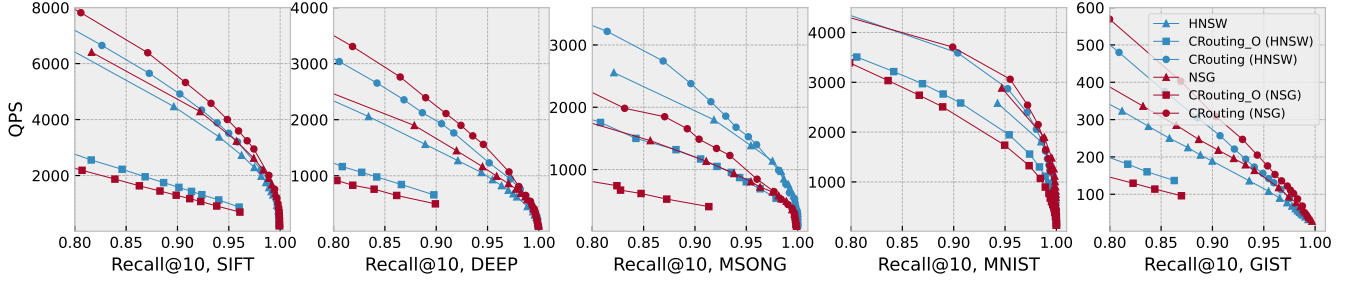


Figure 10: Recall-QPS curves (the top right is better).

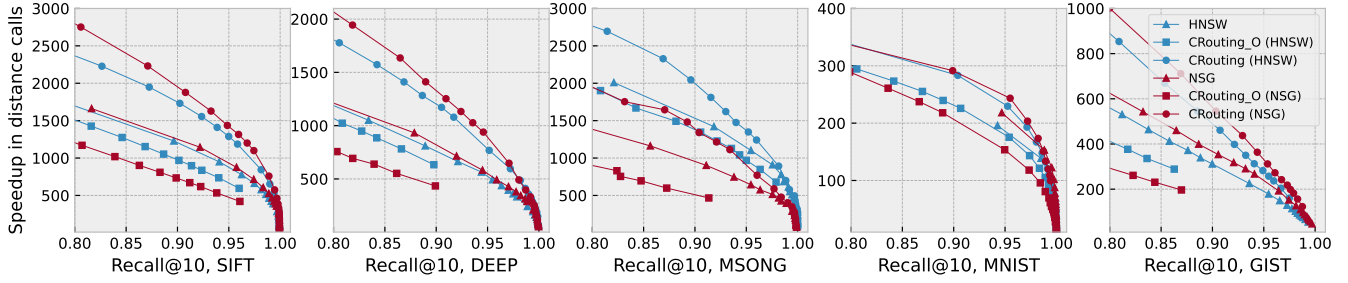


Figure 11: Recall-speedup curves (the top right is better).

Target comparisons. We implement CROUTING on HNSW¹ and NSG², two widely used graph indexes for ANNS in production services like Facebook AI Research [45] and Alibaba e-commerce search [26]. We follow the default parameter settings of their public code. For HNSW, the neighbor limit M for each vector is set to 32 and the insertion candidate neighbor limit efc is set to 256. For NSG, the neighbor limit R is set to 70, the insertion candidate neighbor limit C is set to 500, and the insertion priority queue length L is set to 60. We first compare CROUTING with initial HNSW and NSG algorithms to demonstrate how CROUTING accelerates them. Then, we compare CROUTING with two currently leading-edge routing strategies including (1) TOGG³, which uses KD-trees to select querying neighbor nodes, and add a fine-tuned step when searching nodes near the query and (2) FINGER⁴, which approximates the distance function in graph-based methods by estimating angles between neighboring residual vectors. Moreover, we evaluate two variants of our systems to distinguish the effect of each proposed design component. Specifically, CROUTING_O refers to the version that only enables the pruning strategy while CROUTING incorporates both pruning and error-correction strategies.

5.2 Improvements over ANNS Algorithms

Figure 10 plots the recall-QPS curves on five datasets. We focus only on the region with the recall at least 80% based on practical needs. Overall, we can observe clearly that CROUTING exhibits the best performance across all datasets. CROUTING improves the QPS of

¹<https://github.com/nmslib/hnswlib>

²<https://github.com/ZJULearning/nsq>

³<https://github.com/whenever5225/TOGG>

⁴<https://github.com/Patrick-H-Chen/FINGER/tree/main>

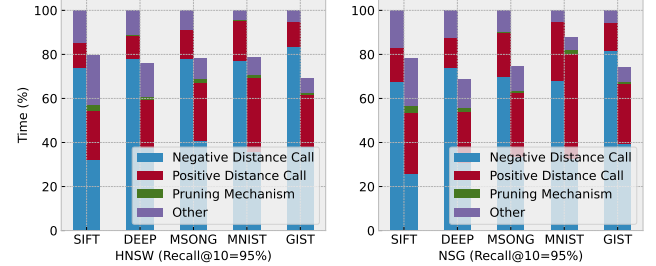


Figure 12: Time cost breakdown. On each dataset, the bar on the left represents the original ANNS algorithms, while the bar on the right represents CROUTING. The time cost is normalized by the cost of the original algorithms.

HNSW and NSG by $1.12\times$ to $1.48\times$ and $1.11\times$ to $1.47\times$, respectively. This demonstrates the effectiveness of our methods. We also find that the performance of CROUTING_O is significantly poor, even falling below the original algorithms. This indicates that relying solely on the pruning strategy is insufficient, as it results in the incorrect deletion of a large number of nodes.

To further analyze the reasons behind the performance improvement, we show the detailed recall-speedup curves in Figure 11. The recall-speedup curves display a trend similar to the recall-QPS curves. CROUTING achieves a speedup in distance calls ranging from $1.22\times$ to $1.58\times$ compared to HNSW, and from $1.15\times$ to $1.71\times$ compared to NSG, indicating a significant reduction in the number of distance calculations, thereby enhancing the QPS.

Table 3: Performance with varying candidate array sizes on the DEEP dataset. Hop means the number of distance calls.

efs	HNSW		CRouting_O		CRouting	
	Recall	Hop	Recall	Hop	Recall	Hop
30	0.889	1234651	0.204	233588	0.676	413111
40	0.921	1507433	0.256	253973	0.753	489692
60	0.954	2032356	0.340	291073	0.842	635833
80	0.970	2534864	0.407	325629	0.886	779403
100	0.978	3013367	0.453	358959	0.917	926499
200	0.994	5194785	0.620	518164	0.972	1678470
300	0.997	7143884	0.708	672941	0.986	2431958
400	0.998	8934851	0.772	825041	0.992	3174724
500	0.999	10624804	0.808	977380	0.995	3909369
700	0.999	13772090	0.866	1279024	0.998	5343785
900	0.999	16686444	0.897	1578669	0.998	6736528

Moreover, we decompose the time cost when targeting 95% recall in Figure 12. We observe that CRouting reduces the distance calculation time for negative nodes by 47.4% to 61.6%, supporting our motivation discussed in §2.2. While CRouting introduces additional checks for the pruning mechanism, it still reduces the overall running time by 12.4% to 31.4%. The pruning mechanism accounts for only 0.7% to 3.9% of the total time. This low overhead is primarily due to the fact that a single cosine calculation involves only a few multiplications and additions. In contrast, calculating the exact distance for a d -dimensional vector requires d multiplications, $d - 1$ additions, and a single random memory read operation. Thus, the pruning algorithm results in significant performance gains.

5.3 Ablation Study

The accuracy and performance of the greedy search can vary depending on the size of the candidate array efs (see Algorithm 1). Table 3 illustrates the recall@10 and hop (i.e., the number of distance calls) for different values of efs . When efs equals 100 (highlighted in pink), CRouting_O reduces the number of hops by 90% of the original greedy search algorithm, but at the cost of a significant drop in recall (from 97% to 45%). In contrast, enabling the error-correction technique allows CRouting to achieve 91% recall. Although this results in more hops than CRouting_O, CRouting still reduces the number of hops by 70% compared to the original greedy search.

The pruning strategy sacrifices accuracy for performance, ensuring a substantial reduction in the number of distance calls. On the other hand, the error-correction strategy sacrifices performance for improved accuracy. Because the revisited nodes have a higher likelihood of being positive nodes, it is worthwhile to recalculate their distances. By combining both techniques, CRouting achieves a better balance between performance and accuracy. For instance, when recall reaches around 89% (highlighted in purple), CRouting reduces the number of hops by 36.9% compared to the original greedy search, and by 50.6% compared to CRouting_O.

5.4 Error Analysis

Although we cannot mathematically prove the approximation error bounds of CRouting, we assess two accuracy metrics: relative error and the incorrect pruning ratio, to empirically verify that its

Table 4: Average relative error of CRouting.

	SIFT	DEEP	MSONG	MNIST	GIST
HNSW	7.00%	6.25%	6.71%	6.82%	5.14%
NSG	6.84%	5.54%	6.47%	6.93%	5.07%

Table 5: The ratio of incorrect pruning of CRouting.

	SIFT	DEEP	MSONG	MNIST	GIST
HNSW	3.91%	4.16%	3.46%	2.44%	5.83%
NSG	3.46%	3.24%	4.70%	2.48%	5.37%

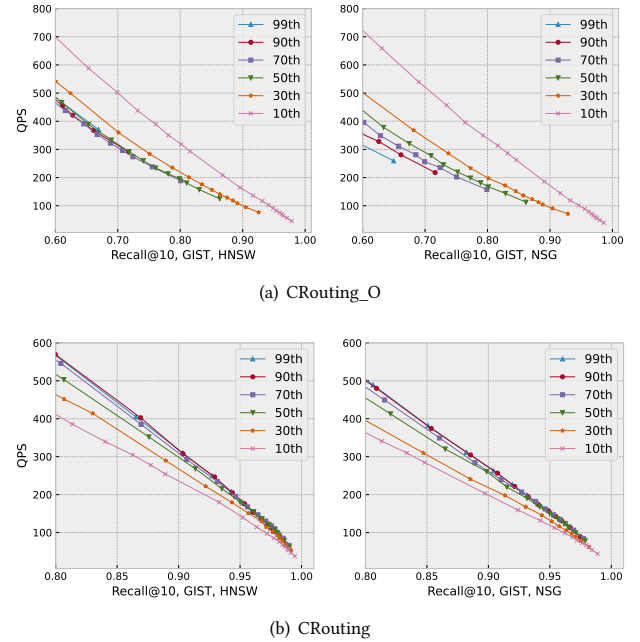


Figure 13: Effect of the pruning threshold.

accuracy is acceptable. Table 4 presents the relative error between the estimated distance $D_{estimated}$ and the true distance D_{true} . The relative error is defined as $e = \frac{|D_{true} - D_{estimated}|}{D_{true}}$. The average relative error of CRouting is approximately 6%. Additionally, Table 5 displays the number of false negatives, where nodes incorrectly classified as negative are actually positive. The maximum ratio of incorrect pruning remains below 6% across all datasets. These results demonstrate the effectiveness of CRouting in distance estimation.

5.5 Sensitive Analysis

The only parameter introduced by CRouting is the pruning threshold (i.e., the value of θ). Other parameters, such as the number of neighbors, M and R , and result number K , are inherent to the graph-based ANNS algorithms and are set based on dataset dimensions, accuracy requirements, and latency constraints.

Effect of the pruning threshold. Figure 13 illustrates the impact of varying the pruning threshold by adjusting the angle from the 10th to the 99th percentile of the angle distribution. Larger

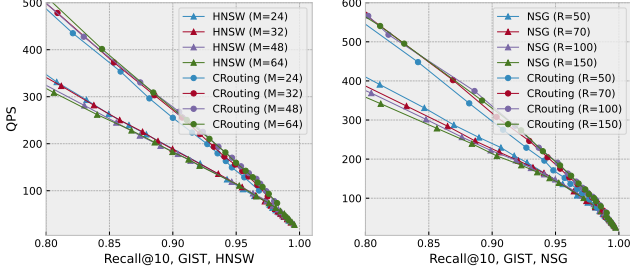


Figure 14: Effect of the number of connected neighbors.

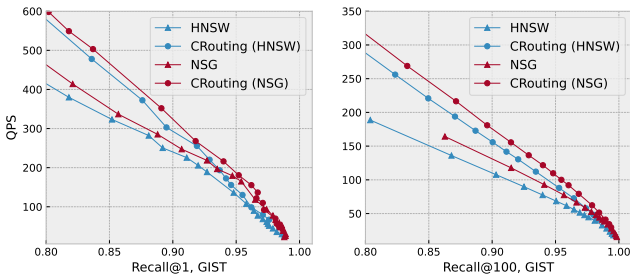
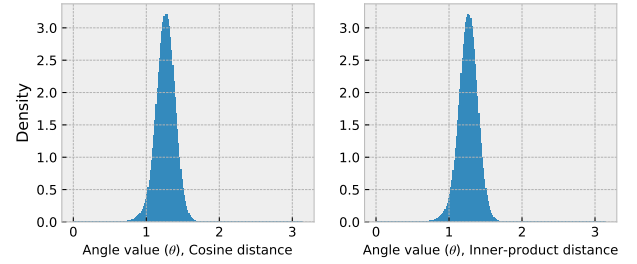


Figure 15: Effect of different result numbers.

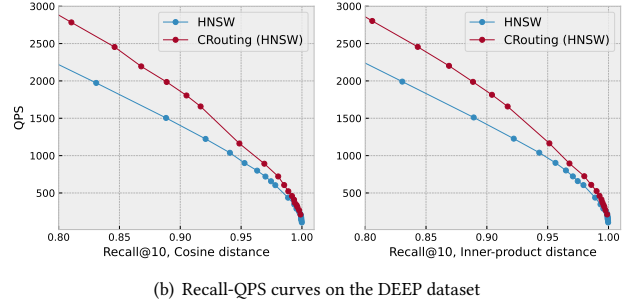
angles for CRouting_O generally result in lower performance. In contrast, for CRouting with error-correction technique enabled, selecting a larger angle typically leads to improved performance. This is because larger angles aggressively prune more nodes, which enhances the QPS. Although this increases the likelihood of mistakenly pruning some nodes, the accuracy loss from such errors can be mitigated by our error-correction mechanism. Across all datasets and algorithms, we consistently observe the best performance at the 90th percentile. Consequently, we set the pruning threshold to the angle value at 90th percentile.

Effect of the number of neighbors. The parameters M and R control the number of connected neighbors on HNSW and NSG algorithms, respectively, and this number directly influences the overall size of the graph. In practical applications, users often adjust the number of neighbors based on their memory capacity and recall requirements. Figure 14 shows the recall-QPS curves of CRouting on the GIST dataset with varying numbers of neighbors. CRouting consistently enhances QPS in all scenarios. Additionally, we find that as the number of neighbors increases, the performance improvements brought by CRouting become more pronounced. As the dimensionality of real-world data increases, more complex and intricate graphs are needed to achieve high recall [26, 55]. This inevitably increases the number of connected neighbors, making our approach more attractive.

Effect of the result number. The parameter K in Recall@ K represents the result number. Figure 15 shows the recall-QPS curves for $K = 1$ and $K = 100$ on the GIST dataset. As K increases, the routing becomes more challenging, yet CRouting consistently accelerates the search by at least 30% when targeting 80% recall, demonstrating its robustness across different K .

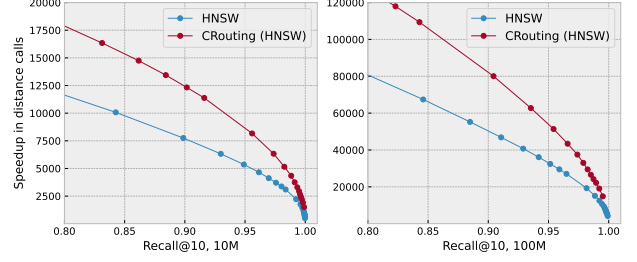


(a) Probability density of angles on the DEEP dataset

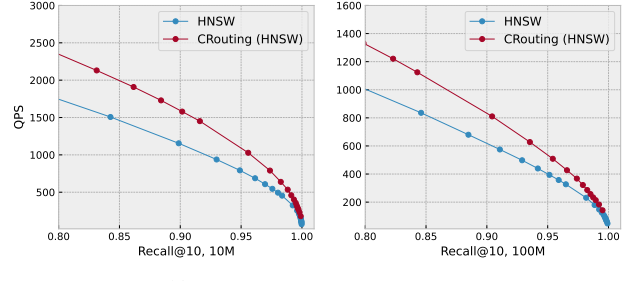


(b) Recall-QPS curves on the DEEP dataset

Figure 16: Generality across different distance metrics.



(a) Recall-speedup curves on large datasets



(b) Recall-QPS curves on large datasets

Figure 17: Scalability across different data volumes.

5.6 Generality and Scalability

Other distance metrics. We assess the generality of CRouting for cosine and inner-product distance metrics. Figure 16(a) shows that the angle distributions with other metrics are similar to that of the

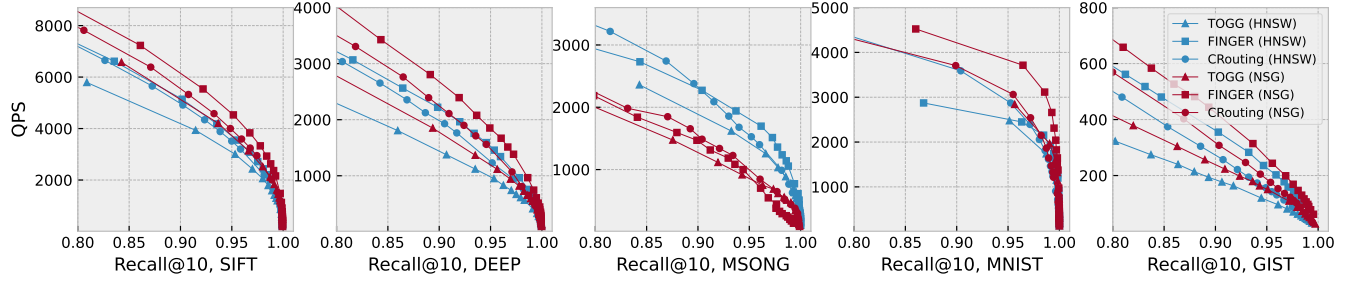


Figure 18: Recall-QPS curves for various routing strategies (the top right is better).

Table 6: Construction time (sec) for various routing strategies.

Dataset	HNSW	+TOGG	+FINGER	+CRouting
SIFT	677.1	707.8 (+5%)	771.7 (+14%)	685.9 (+1%)
DEEP	1163.1	1241.7 (+7%)	1397.1 (+20%)	1168.1 (+1%)
MSONG	1441.9	1508.6 (+5%)	1702.6 (+18%)	1461.8 (+1%)
MNIST	46.1	49.2 (+7%)	81.6 (+78%)	46.5 (+1%)
GIST	2881.8	3014.7 (+5%)	3614.9 (+25%)	2903.3 (+1%)
Dataset	NSG	+TOGG	+FINGER	+CRouting
SIFT	163.1	193.6 (+19%)	249.4 (+53%)	169.1 (+4%)
DEEP	265.2	350.8 (+32%)	474.5 (+79%)	272.3 (+3%)
MSONG	317.8	389.9 (+23%)	589.6 (+86%)	325.7 (+2%)
MNIST	13.8	16.6 (+20%)	45.1 (+226%)	14.3 (+4%)
GIST	806.9	960.4 (+19%)	1546.3 (+92%)	814.4 (+1%)

Table 7: Index size (MB) for various routing strategies.

Dataset	HNSW	+TOGG	+FINGER	+CRouting
SIFT	751.8	767.1 (+2%)	2968.2 (+295%)	873.8 (+16%)
DEEP	1240.1	1255.4 (+1%)	3456.5 (+178%)	1362.1 (+10%)
MSONG	1851.3	1866.4 (+1%)	4050.5 (+119%)	1972.4 (+7%)
MNIST	195.2	196.2 (+1%)	328.3 (+68%)	202.5 (+4%)
GIST	3925.6	3940.9 (+1%)	6142.1 (+56%)	4047.7 (+3%)
Dataset	NSG	+TOGG	+FINGER	+CRouting
SIFT	620.8	636.2 (+3%)	3264.5 (+426%)	745.8 (+21%)
DEEP	1142.1	1157.3 (+1%)	3785.7 (+232%)	1299.8 (+14%)
MSONG	1688.2	1703.3 (+1%)	4311.4 (+156%)	1778.9 (+5%)
MNIST	184.4	185.3 (+1%)	343.1 (+86%)	188.7 (+3%)
GIST	3747.4	3762.7 (+1%)	6818.4 (+82%)	3825.1 (+2%)

Euclidean distance. Using other distance metrics does not change the directional randomness between a node and its neighbors, and the angular distribution still exhibits a skewed characteristic. Therefore, the pruning strategy of CRouting remains effective. As shown in Figure 16(b), CRouting achieves consistent improvements in QPS across different distance metrics.

Search on large datasets. We evaluate the scalability of CRouting in terms of data volume by sampling 10 million and 100 million vectors from the SIFT-1B dataset [1]. The SIFT-100M dataset represents the largest dataset that can be processed on our machine. Figure 17 shows the recall-speedup and recall-QPS curves. The results demonstrate that CRouting consistently outperforms the baseline algorithms across all data volumes.

5.7 Comparison to Previous Routing Strategies

Figure 18 illustrates the recall-QPS curves for various routing strategies, with all competitors employing consistent index parameters. Across all datasets, TOGG exhibits the poorest performance. This is primarily due to the use of the KD-tree for filtering out neighbors that differ in direction from the query node, which is often inaccurate in high-dimensional spaces, as confirmed by previous research [75]. Both CRouting and FINGER achieve higher QPS than TOGG. Although FINGER's QPS is approximately 10% higher than CRouting, it requires more construction time and incurs higher space costs for graph construction.

From the results presented in Table 6, we observe that the construction time of CRouting increases by no more than 1% on the HNSW algorithm and by no more than 4% on the NSG algorithm.

Conversely, the construction time of FINGER increases by 14% to 78% on the HNSW algorithm, and increases by 53% to 226% on the NSG algorithm. FINGER requires more indexing time due to the need to construct an additional subspace for each node. This also explains why it has a higher QPS, as a substantial portion of the computational tasks during the search phase are offloaded to the construction process. Table 7 shows the results of index size. The memory footprint of CRouting increases by 2% to 21% due to the requirement to store the distances to neighboring nodes. FINGER incurs pronounced space costs to store the information about projected vectors and LSH. Specifically, the memory overhead of FINGER increases by 56% to 295% on the HNSW algorithm and by 82% to 426% on the NSG algorithm.

Construction time and space are critical performance metrics in vector databases. Indexes for vector search are typically rebuilt weekly [49] to balance low query latency, high accuracy, and the daily updates of billions of vectors. However, the process of graph reconstruction incurs significant resource overhead. For instance, building a global graph-based index for a 128 GB, 128-dimensional SIFT dataset with 1 billion vectors requires 1100 GB of memory over 2 days, or 5 days with 64 GB of memory and 32 vCPUs [69]. FINGER significantly increases both construction time and index size, making it particularly costly in such scenarios. CRouting exhibits strong competitiveness in both construction and query efficiency for graph-based ANNS algorithms, making it a compelling choice for routing strategies.

6 Related Work

Approximate Nearest Neighbor Search (ANNS). Existing ANNS algorithms can be categorized into four main types: (1) graph-based methods [25, 26, 39, 52, 54, 55, 58, 69], (2) quantization-based methods [7, 8, 29–31, 34, 37, 43], (3) tree-based methods [5, 12, 16, 18, 19, 57, 63, 67], and (4) hashing-based methods [20, 27, 33, 40, 50, 53, 70, 71, 80]. Notably, graph-based approaches demonstrate superior performance for in-memory ANNS. In contrast, quantization-based methods excel in scenarios with limited memory resources. Additionally, a substantial body of research has explored the application of machine learning techniques to accelerate searches [10, 21, 23, 48, 61]. For further details, we direct readers to recent tutorials [22, 62, 72], as well as comprehensive reviews and benchmarks [6, 13, 52, 60, 75].

Routing strategies. TOGG [76] and HCNG [58] utilize KD-trees to ascertain the direction of the query, effectively narrowing the search to vectors aligned with that specified direction. FIN-GER [15] leverages Locality Sensitive Hashing to estimate the distance of each neighbor from the query. Additionally, other machine learning-based optimizations [4, 10, 38, 48, 51, 61] develop a routing function that employs supplementary representations to enhance routing efficiency from the starting node to the nearest neighbor. However, all these optimizations either sacrifice search accuracy or require extra computational resources, resulting in prolonged graph construction times. In contrast, CRouting strikes a favorable balance between search and construction efficiency.

Other Optimizations. As the volume of vector data continues to increase, there has been a surge in interest around supporting incremental updates to vector indexes [56, 68, 77], a crucial technique for enabling efficient and accurate for ANNS. Some studies [32, 74] focus on developing efficient and robust frameworks for hybrid query processing, which integrates ANNS with attribute constraints. Additionally, several efforts have optimized ANNS for newer hardware. For example, GPU-based ANN indexes such as SONG [79] and GGNN [36] have been proposed, achieving up to two orders of magnitude speedup over CPU-based methods. HM-ANN [64] redesigns the HNSW algorithm using Intel Optane persistent memory [59]. CXL-ANNS [42] decouples DRAM from the host via Compute Express Link [17], placing all essential datasets into its memory pool to handle billion-point graph-based ANNS. FANNS [44] automatically co-designs hardware and algorithms on FPGAs based on user-defined recall requirements and hardware resource budgets. These advanced optimizations are orthogonal to our work and can be incorporated in future research efforts.

7 Conclusions

We propose CRouting, a novel routing strategy designed to enhance navigation in graph-based ANNS algorithms. CRouting approximates the distance function by leveraging the angle distributions of high-dimensional vectors, enabling the avoidance of unnecessary distance calculations. It is designed as a plugin to optimize existing graph-based search with minimal code modifications. Our experiments show that CRouting reduces the number of distance computations by up to 41.5% across two state-of-the-art algorithms, HNSW and NSG, while maintaining the same accuracy, thereby enhancing the overall QPS by up to 1.48×.

References

- [1] Anon. 2010. Datasets for approximate nearest neighbor search. <http://corpus-texmex.irisa.fr/>. Last accessed on Sep-2024.
- [2] Anon. 2011. Million Song Dataset Benchmarks. <http://www.ifs.tuwien.ac.at/mir/msd/>. Last accessed on Sep-2024.
- [3] Anon. 2018. Deep1M Dataset. <https://www.cse.cuhk.edu.hk/systems/hash/gqr/datasets.html>. Last accessed on Sep-2024.
- [4] Matej Antol, Jaroslav Ol'ha, Terézia Slanináková, and Vlastislav Dohnal. 2021. Learned metric index—proposition of learned indexing for unstructured data. *Information Systems* 100 (2021), 101774.
- [5] Akhil Arora, Sakshi Sinha, Piyush Kumar, and Arnab Bhattacharya. 2018. Hd-index: Pushing the scalability-accuracy boundary for approximate knn search in high-dimensional spaces. *arXiv preprint arXiv:1804.06829* (2018).
- [6] Martin Aumüller, Erik Bernhardsson, and Alexander Faithfull. 2020. ANN-Benchmarks: A benchmarking tool for approximate nearest neighbor algorithms. *Information Systems* 87 (2020), 101374.
- [7] Artem Babenko and Victor Lempitsky. 2014. Additive quantization for extreme vector compression. In *Proceedings of the IEEE Conference on Computer Vision and Pattern Recognition*. 931–938.
- [8] Artem Babenko and Victor Lempitsky. 2014. The inverted multi-index. *IEEE transactions on pattern analysis and machine intelligence* 37, 6 (2014), 1247–1260.
- [9] Keith Ball et al. 1997. An elementary introduction to modern convex geometry. *Flavors of geometry* 31, 1–58 (1997), 26.
- [10] Dmitry Baranuchi, Dmitry Persiyanov, Anton Sinitin, and Artem Babenko. 2019. Learning to route in similarity graphs. In *International Conference on Machine Learning*. PMLR, 475–484.
- [11] Jon Louis Bentley. 1975. Multidimensional binary search trees used for associative searching. *Commun. ACM* 18, 9 (1975), 509–517.
- [12] Alina Beygelzimer, Sham Kakade, and John Langford. 2006. Cover trees for nearest neighbor. In *Proceedings of the 23rd international conference on Machine learning*. 97–104.
- [13] Leonid Boytsov and Bilegsaikhan Naidan. 2013. Engineering efficient and effective non-metric space library. In *Similarity Search and Applications: 6th International Conference, SISAP 2013, A Coruña, Spain, October 2–4, 2013, Proceedings* 6. Springer, 280–293.
- [14] Moses S Charikar. 2002. Similarity estimation techniques from rounding algorithms. In *Proceedings of the thiry-fourth annual ACM symposium on Theory of computing*. 380–388.
- [15] Patrick Chen, Wei-Cheng Chang, Jyun-Yu Jiang, Hsiang-Fu Yu, Inderjit Dhillon, and Cho-Jui Hsieh. 2023. Finger: Fast inference for graph-based approximate nearest neighbor search. In *Proceedings of the ACM Web Conference 2023*. 3225–3235.
- [16] Paolo Ciaccia, Marco Patella, Pavel Zezula, et al. 1997. M-tree: An efficient access method for similarity search in metric spaces. In *Vldb*, Vol. 97. Citeseer, 426–435.
- [17] CXL Consortium. 2020. Cxl specification. <https://computeexpresslink.org/cxl-specification/>. Last accessed on Sep-2024.
- [18] Ryan R Curtin, Parikshit Ram, and Alexander G Gray. 2013. Fast exact max-kernel search. In *Proceedings of the 2013 SIAM International Conference on Data Mining*. SIAM, 1–9.
- [19] Sanjoy Dasgupta and Yoav Freund. 2008. Random projection trees and low dimensional manifolds. In *Proceedings of the fortieth annual ACM symposium on Theory of computing*. 537–546.
- [20] Mayur Datar, Nicole Immorlica, Piotr Indyk, and Vahab S Mirrokni. 2004. Locality-sensitive hashing scheme based on p-stable distributions. In *Proceedings of the twentieth annual symposium on Computational geometry*. 253–262.
- [21] Yihe Dong, Piotr Indyk, Ilya Razenshteyn, and Tal Wagner. 2020. Learning Space Partitions for Nearest Neighbor Search. In *International Conference on Learning Representations*.
- [22] Karima Echihabi, Kostas Zoumpatianos, and Themis Palpanas. 2021. New trends in high-d vector similarity search: al-driven, progressive, and distributed. *Proceedings of the VLDB Endowment* 14, 12 (2021), 3198–3201.
- [23] Chao Feng, Defu Lian, Xiting Wang, Zheng Liu, Xing Xie, and Enhong Chen. 2023. Reinforcement routing on proximity graph for efficient recommendation. *ACM Transactions on Information Systems* 41, 1 (2023), 1–27.
- [24] Myron Flickner, Harpreet Sawhney, Wayne Niblack, Jonathan Ashley, Qian Huang, Byron Dom, Monika Gorkani, Jim Hafner, Denis Lee, Dragutin Petkovic, et al. 1995. Query by image and video content: The QBIC system. *computer* 28, 9 (1995), 23–32.
- [25] Cong Fu, Changxu Wang, and Deng Cai. 2021. High dimensional similarity search with satellite system graph: Efficiency, scalability, and unindexed query compatibility. *IEEE Transactions on Pattern Analysis and Machine Intelligence* 44, 8 (2021), 4139–4150.
- [26] Cong Fu, Chao Xiang, Changxu Wang, and Deng Cai. 2019. Fast approximate nearest neighbor search with the navigating spreading-out graph. *Proceedings of the VLDB Endowment* 12, 5 (2019), 461–474.
- [27] Junhao Gan, Jianlin Feng, Qiong Fang, and Wilfred Ng. 2012. Locality-sensitive hashing scheme based on dynamic collision counting. In *Proceedings of the 2012*

ACM SIGMOD international conference on management of data. 541–552.

[28] Jianyang Gao and Cheng Long. 2023. High-dimensional approximate nearest neighbor search: with reliable and efficient distance comparison operations. *Proceedings of the ACM on Management of Data* 1, 2 (2023), 1–27.

[29] Jianyang Gao and Cheng Long. 2024. RaBitQ: Quantizing High-Dimensional Vectors with a Theoretical Error Bound for Approximate Nearest Neighbor Search. *Proceedings of the ACM on Management of Data* 2, 3 (2024), 1–27.

[30] Tiezheng Ge, Kaiming He, Qifa Ke, and Jian Sun. 2013. Optimized product quantization. *IEEE transactions on pattern analysis and machine intelligence* 36, 4 (2013), 744–755.

[31] Tiezheng Ge, Kaiming He, Qifa Ke, and Jian Sun. 2013. Optimized product quantization for approximate nearest neighbor search. In *Proceedings of the IEEE conference on computer vision and pattern recognition*, 2946–2953.

[32] Siddharth Gollapudi, Neel Karia, Varun Sivashankar, Ravishankar Krishnaswamy, Nikit Begwani, Swapnil Raz, Yiyong Lin, Yin Zhang, Neelan Mahapatro, Premkumar Srinivasan, et al. 2023. Filtered-diskann: Graph algorithms for approximate nearest neighbor search with filters. In *Proceedings of the ACM Web Conference 2023*, 3406–3416.

[33] Long Gong, Huayi Wang, Mitsunori Ogihara, and Jun Xu. 2020. iDEC: indexable distance estimating codes for approximate nearest neighbor search. *Proceedings of the VLDB Endowment* 13, 9 (2020).

[34] Yunchao Gong, Svetlana Lazebnik, Albert Gordo, and Florent Perronnin. 2012. Iterative quantization: A procrustean approach to learning binary codes for large-scale image retrieval. *IEEE transactions on pattern analysis and machine intelligence* 35, 12 (2012), 2916–2929.

[35] Adrien Grand. 2023. Vector search in Elasticsearch: The rationale behind the design. <https://www.elastic.co/search-labs/blog/vector-search-elasticsearch-rationale>. Last accessed on Sep-2024.

[36] Fabian Groh, Lukas Ruppert, Patrick Wieschollek, and Hendrik PA Lensch. 2022. Ggnn: Graph-based gpu nearest neighbor search. *IEEE Transactions on Big Data* 9, 1 (2022), 267–279.

[37] Ruiqi Guo, Philip Sun, Erik Lindgren, Quan Geng, David Simcha, Felix Chern, and Sanjiv Kumar. 2020. Accelerating large-scale inference with anisotropic vector quantization. In *International Conference on Machine Learning*. PMLR, 3887–3896.

[38] Gaurav Gupta, Tharun Medini, Anshumali Shrivastava, and Alexander J Smola. 2022. Bliss: A billion scale index using iterative re-partitioning. In *Proceedings of the 28th ACM SIGKDD Conference on Knowledge Discovery and Data Mining*, 486–495.

[39] Ben Harwood and Tom Drummond. 2016. Fannn: Fast approximate nearest neighbour graphs. In *Proceedings of the IEEE Conference on Computer Vision and Pattern Recognition*, 5713–5722.

[40] Qiang Huang, Jianlin Feng, Yikai Zhang, Qiong Fang, and Wilfred Ng. 2015. Query-aware locality-sensitive hashing for approximate nearest neighbor search. *Proceedings of the VLDB Endowment* 9, 1 (2015), 1–12.

[41] Piotr Indyk and Rajeev Motwani. 1998. Approximate nearest neighbors: towards removing the curse of dimensionality. In *Proceedings of the thirtieth annual ACM symposium on Theory of computing*, 604–613.

[42] J Jang, H Choi, H Bae, S Lee, M Kwon, and M Jung. 2023. CXL-ANNS: Software-Hardware Collaborative Memory Disaggregation and Computation for Billion-Scale Approximate Nearest Neighbor Search. In *2023 USENIX Annual Technical Conference (USENIX ATC 23)*. USENIX Association.

[43] Hervé Jegou, Matthijs Douze, and Cordelia Schmid. 2010. Product quantization for nearest neighbor search. *IEEE transactions on pattern analysis and machine intelligence* 33, 1 (2010), 117–128.

[44] Wensi Jiang, Shigang Li, Yu Zhu, Johannes de Fine Licht, Zhenhao He, Runbin Shi, Cedric Renggli, Shuai Zhang, Theodoros Rekatsinas, Torsten Hoefer, et al. 2023. Co-design hardware and algorithm for vector search. In *Proceedings of the International Conference for High Performance Computing, Networking, Storage and Analysis*, 1–15.

[45] Jeff Johnson, Matthijs Douze, and Hervé Jégou. 2019. Billion-scale similarity search with GPUs. *IEEE Transactions on Big Data* 7, 3 (2019), 535–547.

[46] Yann LeCun, Corinna Cortes, and Christopher J.C. Burges. 1998. The MNIST Database of Handwritten Digits. <http://yann.lecun.com/exdb/mnist/>. Last accessed on Sep-2024.

[47] Patrick Lewis, Étahn Perez, Aleksandra Piktus, Fabio Petroni, Vladimir Karpukhin, Naman Goyal, Heinrich Küttler, Mike Lewis, Wen-tau Yih, Tim Rocktäschel, et al. 2020. Retrieval-augmented generation for knowledge-intensive nlp tasks. *Advances in Neural Information Processing Systems* 33 (2020), 9459–9474.

[48] Conglong Li, Minjia Zhang, David G Andersen, and Yuxiong He. 2020. Improving approximate nearest neighbor search through learned adaptive early termination. In *Proceedings of the 2020 ACM SIGMOD International Conference on Management of Data*, 2539–2554.

[49] Jie Li, Haifeng Liu, Chuanghua Gui, Jianyu Chen, Zhenyuan Ni, Ning Wang, and Yuan Chen. 2018. The design and implementation of a real time visual search system on JD E-commerce platform. In *Proceedings of the 19th International Middleware Conference Industry*, 9–16.

[50] Jinfeng Li, Xiao Yan, Jian Zhang, An Xu, James Cheng, Jie Liu, Kelvin KW Ng, and Ti-chung Cheng. 2018. A general and efficient querying method for learning to hash. In *Proceedings of the 2018 International Conference on Management of Data*, 1333–1347.

[51] Lingli Li, Ao Han, Xiaotong Cui, and Baohua Wu. 2024. Flex: a fast and light-weight learned index for KNN search in high-dimensional space. *Information Sciences* 669 (2024), 120546.

[52] Wen Li, Ying Zhang, Yifang Sun, Wei Wang, Mingjie Li, Wenjie Zhang, and Xuemin Lin. 2019. Approximate nearest neighbor search on high dimensional data—experiments, analyses, and improvement. *IEEE Transactions on Knowledge and Data Engineering* 32, 8 (2019), 1475–1488.

[53] Kejing Lu, Hongya Wang, Wei Wang, and Mineichi Kudo. 2020. VHP: approximate nearest neighbor search via virtual hypersphere partitioning. *Proceedings of the VLDB Endowment* 13, 9 (2020), 1443–1455.

[54] Yury Malkov, Alexander Ponomarenko, Andrey Logvinov, and Vladimir Krylov. 2014. Approximate nearest neighbor algorithm based on navigable small world graphs. *Information Systems* 45 (2014), 61–68.

[55] Yury Malkov and Dmitry A Yashunin. 2018. Efficient and robust approximate nearest neighbor search using hierarchical navigable small world graphs. *IEEE transactions on pattern analysis and machine intelligence* 42, 4 (2018), 824–836.

[56] Jason Mohoney, Anil Pacaci, Shihabur Rahman Chowdhury, Umar Farooq Minhas, Jeffery Pound, Cedric Renggli, Nima Reyhani, Ihab F Ilyas, Theodoros Rekatsinas, and Shivaram Venkataraman. 2024. Incremental IVF Index Maintenance for Streaming Vector Search. *arXiv preprint arXiv:2411.00970* (2024).

[57] Marius Muja and David G Lowe. 2014. Scalable nearest neighbor algorithms for high dimensional data. *IEEE transactions on pattern analysis and machine intelligence* 36, 11 (2014), 2227–2240.

[58] Javier Vargas Munoz, Marcos A Gonçalves, Zanoni Dias, and Ricardo da S Torres. 2019. Hierarchical clustering-based graphs for large scale approximate nearest neighbor search. *Pattern Recognition* 96 (2019), 106970.

[59] Intel Newsroom. 2019. Intel® Optane™ DC Persistent Memory. <https://www.intel.com/content/www/us/en/products/memory-storage/optane-dc-persistent-memory.html>. Last accessed on Sep-2024.

[60] Marco Patella and Paolo Ciaccia. 2009. Approximate similarity search: A multi-faceted problem. *Journal of Discrete Algorithms* 7, 1 (2009), 36–48.

[61] Liudmila Prokhorenkova and Aleksandr Shekhovtsov. 2020. Graph-based nearest neighbor search: From practice to theory. In *International Conference on Machine Learning*. PMLR, 7803–7813.

[62] Jianbin Qin, Wei Wang, Chuan Xiao, Ying Zhang, and Yaoshu Wang. 2021. High-dimensional similarity query processing for data science. In *Proceedings of the 27th ACM SIGKDD Conference on Knowledge Discovery & Data Mining*, 4062–4063.

[63] Parikshit Ram and Kaushik Sinha. 2019. Revisiting kd-tree for nearest neighbor search. In *Proceedings of the 25th ACM SIGKDD international conference on knowledge discovery & data mining*, 1378–1388.

[64] Jie Ren, Minjia Zhang, and Dong Li. 2020. Hm-ann: Efficient billion-point nearest neighbor search on heterogeneous memory. *Advances in Neural Information Processing Systems* 33 (2020), 10672–10684.

[65] Badrul Sarwar, George Karypis, Joseph Konstan, and John Riedl. 2001. Item-based collaborative filtering recommendation algorithms. In *Proceedings of the 10th international conference on World Wide Web*, 285–295.

[66] Zhitao Shen, Shiyu Yang, Weibo Chen, Kunming Wang, Yue Li, Jiabao Jin, Wei Jia, Junwei Chen, Yuan Su, Xiaoxia Duan, Wei Chen, Lei Wang, Jie Song, Ruoyi Ruan, and Xuemin Lin. 2025. TierBase: A Workload-Driven Cost-Optimized Key-Value Store . In *2025 IEEE 41st International Conference on Data Engineering (ICDE)*. IEEE Computer Society, 571–584.

[67] Chanop Silpa-Anan and Richard Hartley. 2008. Optimised KD-trees for fast image descriptor matching. In *2008 IEEE Conference on Computer Vision and Pattern Recognition*. IEEE, 1–8.

[68] Aditi Singh, Suhas Jayaram Subramanya, Ravishankar Krishnaswamy, and Harsha Vardhan Simhadri. 2021. Freshdiskann: A fast and accurate graph-based ann index for streaming similarity search. *arXiv preprint arXiv:2105.09613* (2021).

[69] Suhas Jayaram Subramanya, Devvrit, Rohan Kadekodi, Ravishankar Krishnaswamy, and Harsha Vardhan Simhadri. 2019. DiskANN: fast accurate billion-point nearest neighbor search on a single node. In *Proceedings of the 33rd International Conference on Neural Information Processing Systems*, 13766–13776.

[70] Yifang Sun, Wei Wang, Jianbin Qin, Ying Zhang, and Xuemin Lin. 2014. SRS: solving c-approximate nearest neighbor queries in high dimensional euclidean space with a tiny index. *Proceedings of the VLDB Endowment* (2014).

[71] Yufei Tao, Ke Yi, Cheng Sheng, and Panos Kalnis. 2010. Efficient and accurate nearest neighbor and closest pair search in high-dimensional space. *ACM Transactions on Database Systems (TODS)* 35, 3 (2010), 1–46.

[72] Yao Tian, Ziyang Yue, Ruiyuan Zhang, Xi Zhao, Bolong Zheng, and Xiaofang Zhou. 2023. Approximate Nearest Neighbor Search in High Dimensional Vector Databases: Current Research and Future Directions. *IEEE Data Eng. Bull.* 46, 3 (2023), 39–54.

[73] Jianguo Wang, Xiaomeng Yi, Rentong Guo, Hai Jin, Peng Xu, Shengjun Li, Xiangyu Wang, Xiangzhou Guo, Chengming Li, Xiaohai Xu, et al. 2021. Milvus: A purpose-built vector data management system. In *Proceedings of the 2021 International Conference on Management of Data*, 2614–2627.

[74] Mengzhao Wang, Lingwei Lv, Xiaoliang Xu, Yuxiang Wang, Qiang Yue, and Jiongkang Ni. 2024. An efficient and robust framework for approximate nearest neighbor search with attribute constraint. *Advances in Neural Information Processing Systems* 36 (2024).

[75] Mengzhao Wang, Xiaoliang Xu, Qiang Yue, and Yuxiang Wang. 2021. A comprehensive survey and experimental comparison of graph-based approximate nearest neighbor search. *Proceedings of the VLDB Endowment* 14, 11 (2021), 1964–1978.

[76] Xiaoliang Xu, Mengzhao Wang, Yuxiang Wang, and Dingcheng Ma. 2021. Two-stage routing with optimized guided search and greedy algorithm on proximity graph. *Knowledge-Based Systems* 229 (2021), 107305.

[77] Yuming Xu, Hengyu Liang, Jin Li, Shuotao Xu, Qi Chen, Qianxi Zhang, Cheng Li, Ziyue Yang, Fan Yang, Yuqing Yang, et al. 2023. SPPFresh: Incremental In-Place Update for Billion-Scale Vector Search. In *Proceedings of the 29th Symposium on Operating Systems Principles*, 545–561.

[78] Wen Yang, Tao Li, Gai Fang, and Hong Wei. 2020. Pase: Postgresql ultra-high-dimensional approximate nearest neighbor search extension. In *Proceedings of the 2020 ACM SIGMOD international conference on management of data*, 2241–2253.

[79] Weijie Zhao, Shulong Tan, and Ping Li. 2020. Song: Approximate nearest neighbor search on gpu. In *2020 IEEE 36th International Conference on Data Engineering (ICDE)*. IEEE, 1033–1044.

[80] Bolong Zheng, Zhao Xi, Lianggui Weng, Nguyen Quoc Viet Hung, Hang Liu, and Christian S Jensen. 2020. PM-LSH: A fast and accurate LSH framework for high-dimensional approximate NN search. *Proceedings of the VLDB Endowment* 13, 5 (2020), 643–655.

[81] Xiaoyan Zhong, Haotian Li, Jiabao Jin, Mingyu Yang, Deming Chu, Xiangyu Wang, Zhitao Shen, Wei Jia, George Gu, Yi Xie, et al. 2025. VSAG: An Optimized Search Framework for Graph-based Approximate Nearest Neighbor Search. *arXiv preprint arXiv:2503.17911* (2025).

[82] Chun Jiang Zhu, Tan Zhu, Haining Li, Jinbo Bi, and Minghu Song. 2019. Accelerating large-scale molecular similarity search through exploiting high performance computing. In *2019 IEEE International Conference on Bioinformatics and Biomedicine (BIBM)*. IEEE, 330–333.